



## A channel sampling strategy for measurement of mineral modal and chemical composition of drill cores: application to lower oceanic crustal rocks from IODP Expedition 345 to the Hess Deep rift

Robert P. Wintsch<sup>1,2</sup>, Romain Meyer<sup>3</sup>, David L. Bish<sup>4</sup>, Ryan T. Deasy<sup>5</sup>, Toshio Nozaka<sup>6</sup>, and Carley Johnson<sup>7</sup>

<sup>1</sup>Department of Earth and Environmental Sciences, Wesleyan University, Middletown, CT 06459, USA

<sup>2</sup>Connecticut Geological Survey, 79 Elm Street, Hartford, CT 06106-5127, USA

<sup>3</sup>Geological Survey of Luxembourg, Ministry of Mobility and Public Works,  
23, Rue du Chemin de Fer, 8057 Bertrange, Luxembourg

<sup>4</sup>Department of Chemistry, Indiana University, Bloomington, IN 47405, USA

<sup>5</sup>U.S. Geological Survey, Florence Bascom Geoscience Center, 12201 Sunrise Valley Dr.,  
MS 926A, Reston, VA 20192, USA

<sup>6</sup>Department of Earth Sciences, Okayama University, 3-1-1 Tsushima-naka, Okayama 700-8530, Japan

<sup>7</sup>Marathon Oil Corporation, Room #3545, 5555 San Felipe St., Houston, TX 77056, USA

**Correspondence:** Robert P. Wintsch (rwintsch@wesleyan.edu)

Received: 5 November 2021 – Revised: 17 February 2022 – Accepted: 8 April 2022 – Published: 28 October 2022

**Abstract.** We report a new sampling strategy for collecting representative samples of drill core. By splitting the core with a diamond saw into working and archive halves, the saw cuttings constitute a “channel” sample, the best subsample from which to obtain an average mineralogical and geochemical composition of a core. We apply this procedure to sampling core of the lower oceanic crust in the Hess Deep obtained during Expedition 345 of the Integrated Ocean Drilling Program (now International Ocean Discovery Program).

Our results show that particles produced by sawing range from sand to clay sizes. Sand- and silt-sized cuttings can be sampled with a spatula, whereas clay-sized particles remained in suspension after 12 h and could be collected only by settling, aided by centrifuge. X-ray diffraction (XRD) analysis and Rietveld refinement show that phyllosilicates were fractionated into the clay-sized fraction. Thus, collection of both the sedimented fraction and the clay-sized suspended fraction (commonly > 15 wt % of the total) is necessary to capture the whole sample. The strong positive correlation between the recovered sample mass (in grams) and length of core cut demonstrates that this sampling protocol was uniform and systematic, with almost 1.4 g sediment produced per centimeter of core cut. We show that major-element concentrations of our channel samples compare favorably with the compositions of billet-sized samples analyzed aboard the *JOIDES Resolution*, but the results show that individual billet analyses are rarely representative of the whole core recovered. A final test of the validity of our methods comes from the strong positive correlation between the loss on ignition (LOI) values of our channel samples and the H<sub>2</sub>O contents calculated from the modal mineralogy obtained by X-ray diffraction and Rietveld refinement. This sampling procedure shows that grain-sized fractionation modifies both mineralogical and chemical compositions; nevertheless, this channel sampling method is a reliable method of obtaining representative samples of bulk cores. With the ever-increasing precision offered by modern analytical instrumentation, this sampling protocol allows the accuracy of the analytical results to keep pace.

## 1 Introduction

Fundamental questions about the dynamics of plate tectonics require the most statistically robust knowledge of the composition of the oceanic crust produced with variable spreading rates. Slow spreading rates may produce more alkali-rich magmas, whereas fast spreading may produce more mafic magmas with higher percentages of melting (e.g., Regelous et al., 2016). In addition, the state of alteration to hydrated minerals may play an important role in defining the density and seismic properties of the oceanic crust. An understanding of the consequences of the destruction of oceanic crust during subduction at convergent plate margins requires detailed knowledge of the extent of hydration and related alteration mineralogy of the recycled slab. These variables control the flux of fluids returned to the mantle. This in turn affects both petrologic (e.g., hydration melting) and geophysical (e.g., dehydration embrittlement) behavior of these rocks (e.g., Raleigh and Paterson, 1965; Meade and Jeanloz, 1991; Hacker et al., 2003; Bourdon et al., 2003; Manning, 2004; Ranero et al., 2005).

Progress in defining the properties of the oceanic crust has been stymied by the lack of knowledge of the composition of the lower oceanic crust. Our knowledge of the chemical and mineralogical composition of the oceanic crust is biased toward the more accessible volcanic rocks and sheeted dikes from mid-ocean ridge basalt (MORB) (e.g., Stewart et al., 2002, 2005; Blackman et al., 2011; White and Klein, 2014). Analysis of lower crustal lithologies by core and dredged samples provides some answers (e.g., Mével and Stamoudi, 1996; Natland and Dick, 1996; Pedersen et al., 1996; Dick et al., 1999; Manning et al., 1996; Lissenberg et al., 2013), but such studies are limited by small individual sample size and by lack of structural context. In particular, the chemical composition and especially the modal mineralogy of lower plutonic oceanic crust at fast-spreading axes are not as well known as slower spreading centers (Arai and Matsukage, 1996; Coogan et al., 2002; Arai and Takemoto, 2007; Gillis et al., 2014e). There is a large body of literature on the use of reflectance spectroscopy for determining the mineralogy of rocks from the planetary scale (e.g., remote sensing of Mars and Earth) to the microscopic scale. For example, micro-imaging infrared spectroscopy as applied to the Samail ophiolite, Oman (Kelemen et al., 2020), is an advance in detecting whole-core mineralogy but is so far only semi-quantitative. Greenberger et al. (2021) used the X-ray diffraction (XRD) data from Kelemen et al. (2020) to map mineral distributions in oceanic crust from Oman. They were able to determine spatial distributions of a number of minerals and mineral groups in core, with claimed accuracy of 68 %–100 % compared with XRD identifications. Micro-imaging infrared spectroscopy can identify mineral families (Greenberger et al., 2021) with a spatial resolution of  $\sim 250 \mu\text{m}$ , but the method does not discriminate well among important min-

eral groups (e.g., quartz from two feldspars, phyllosilicates, oxides, sulfides, zeolites).

This gap in data from the lower crust was one of the primary motivations for drilling the lowermost ocean crust at the fast-spreading East Pacific Rise on Expedition 345 to the Hess Deep (Gillis et al., 2014e). First-order questions addressed there included (1) what are the compositions of the primitive plutonic rocks that comprise the lower magmatic crust, and (2) what is the state of alteration of that crust? Different approaches used to calculate the bulk major-element compositions of oceanic crust (e.g., Gillis et al., 2014a) are presently still debated (White and Klein, 2014). The major point of contention relates to the composition of the lower oceanic crustal component of the total crust (e.g., Coogan, 2014). Here the lack of quantitative data for the gabbroic lower oceanic crust leads to additional uncertainty.

In this study we describe a sampling strategy that allows us to acquire representative samples of all the cores of lower crustal rocks recovered from Expedition 345 to the Hess Deep. We provide results demonstrating the viability of the sampling method, we present data on the modal mineralogy and major-element compositions of these cores, and we compare our results with those of traditional methods of analyzing centimeter-sized billets subjectively sampled from parts of cores. Deasy et al. (2021) presented the quantitative chemical results of our study and applied them to interpreting magmatic processes in the lower crust and in an updated estimate of the composition of fast-spreading oceanic crust.

## 2 Background on sampling protocols

Samples of oceanic crustal rocks are available from limited coring, dredging, and collecting from submersible dives, but sample size and sample density are typically small, yielding to the conflicting interests and needs of different scientific experiments, as well as to the preservation of the archival half of the core. In the absence of other analytical data, sample selection for chemical analysis is necessarily subjective and as such can be statistically unsystematic. The analysis of a small specimen may be representative of only that particular sample, and extrapolations to the composition of a related outcrop, core, igneous unit, and especially crustal segment can only be made with increasing uncertainty (e.g., Potts, 1987).

Small sample sizes employed for the analysis of hydrothermal alteration are especially limiting. Reactions and structures responsible for alteration have been identified (e.g., Lecuyer and Reynard, 1996; Manning and MacLeod, 1996; Manning et al., 1996; Frost et al., 2008; Meyer et al., 2013; Deasy et al., 2014; Nozaka and Fryer, 2011; Marks et al., 2013, 2014; Nozaka et al., 2016, 2017), but their net effect on modifying the bulk mineralogy of the protolith is not well understood (e.g., Gillis et al., 2005) and stands to be improved. In fact, no analyst, with even the best analytical methods, will be able to correct data for errors related

to unsystematic sampling (Heinrichs and Hermann, 1990). An analysis of an entire core comes much closer to producing the data needed to assess the effects of alteration on bulk compositions.

Representative sampling strategies are well established in geochemical ore prospecting (e.g., Heinrichs and Hermann, 1990). Linear sampling, i.e., channel sampling, provides representative samples for mineralogy and chemical analysis (Sinclair and Blackwell, 2002), and such linear sampling has been widely applied in the metal mining and coal industries (e.g., Agterberg, 2012; Stanton, 1986; Swanson and Huffman, 1976). In surface exposures this involves cutting a linear channel, typically 10 cm deep, across the fresh outcrop face (Cornish, 1966). The exact shape of the channel has little influence on the sample quality, but a uniform volume of sample needs to be guaranteed over the total length of the channel (Heinrichs and Hermann, 1990). An additional representative sampling method in ore prospecting equivalent to a channel sample is the “Bohrmehlprobe”, where the fine-grained material obtained from drilling rock-blasting holes is collected for analysis (Heinrichs and Hermann, 1990). NASA has recently used a similar drilling sampling strategy with the Curiosity rover on Mars for quantitative mineral compositions with the CheMin instrument (Bish et al., 2004, 2013). Finally, Hart et al. (1999) followed the philosophy of a linear channel sample within the scientific drilling community by trimming a 1 cm wide wedge off the edges of several lengths of Ocean Drilling Program (ODP) core. Their highly successful “strip” sample did produce representative samples of core, but it also consumed a large percentage of the precious core recovered and so was never repeated within the ocean drilling programs.

Identifying a sample representative of the mineral or chemical composition of an entire length of core was especially challenging for the recent IODP Expedition 345, Site U1415, to the Hess Deep for several reasons. First, the billets (typically  $2 \times 3 \times 3$  cm, 15 to 30 g) used in chemical analysis (Gillis et al., 2014d) are too small to adequately sample the many varieties of gabbroic rocks that contained oikocrysts of clinopyroxene up to 5 cm in diameter. The same is true for samples with modal variations and layering that occur on the scale of up to 10 cm (Gillis et al., 2014d; Koepke et al., 2013). The most limiting property of the core is the heterogeneous distribution of alteration. It is typically associated with fractures and faults whose occurrence is equally heterogeneous, and the scales of alteration vary from micrometers to meters in width. The scale and distribution of these structures is much too large to be captured proportionally in typical IODP sample pieces, and the alteration typically dismembers the core into irregular-sized pieces. Moreover, billets are typically cut from well-indurated core, thereby biasing sampling against altered material. Thus, the analysis of billets cannot be representative of the bulk rock or even the drilled units.

Another uncertainty in the study of IODP cores stems from the method of obtaining modal mineralogy. Modal mineralogy is typically determined by “visual core descriptions” (VCDs; Gillis et al., 2014c), where a scientist estimates by eye the volume percent of each magmatic and alteration mineral. These are subject to uncertainties derived from the several scientists involved in both identifying the mineralogy correctly and in estimating modal percentages of each mineral accurately. These errors are not systematic, because six or more scientists may be involved in the estimate of magmatic and alteration mineralogy of the many pieces of core. In addition, it is often difficult, if not impossible, to obtain an accurate identification let alone an accurate modal estimate of fine-grained alteration minerals. It is well known from oil reservoir characterization studies that visual estimates are often twice as high as point-counted values (Lucia, 2007). As a result, visual estimates can be inaccurate if not calibrated with point-counted methods.

Here we describe a new method of obtaining a representative sample of hard-rock core: a channel sample of the drill core. These samples were obtained by meticulously collecting all of the cuttings, slurries, and rinse water from the linear or “channel sample” of the core produced by the saw as it cut each of the 42 cores into working and archive halves on IODP Expedition 345 to the Hess Deep (Gillis et al., 2014c). A distinct advantage of this method is that it did not consume any new volume of core. These representative samples were then used to determine (1) the modal mineralogy by collecting X-ray powder diffraction data and using Rietveld refinement methods to determine the total wt % of each mineral (Wintsch et al., 2013), (2) the major- and trace-element compositions (Deasy et al., 2021), and (3) Sr isotopic compositions (Deasy et al., 2014; Wintsch et al., 2019). This new method has distinct advantages over traditional methods used in past IODP expeditions as described below.

### 3 Methods

In this section we provide detail on new methods of channel sampling, i.e., the systematic collection of rock material removed during the separation of cores into working and archive halves. The chemical analytical methods are described in Deasy et al. (2021). During IODP Expedition 345, 42 cores were recovered “in situ” with the label “R.” Other samples were of rock that collapsed into the hole and commonly produced “pebbly” material, having been ground by the rotary drilling process. These “ghost” or “G” samples (Gillis et al., 2014c) were maintained but were not systematically sampled in this study, because their position in the hole could not be firmly established. The results of these mineralogical and chemical analyses confirm that this is a robust method of sample collection.

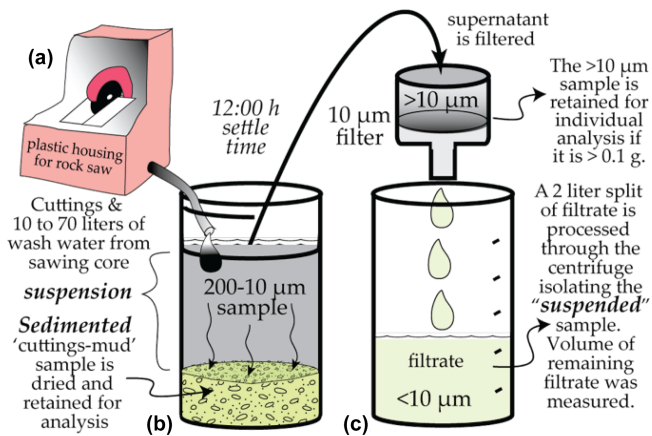


**Figure 1.** A schematic diagram showing the processes involved in collecting the channel sample of the drill core. Larger particles produced in cutting the core (a) are sedimented in the plastic housing, whereas smaller particles are flushed into a large carboy (b). A coarser-grained sedimented subsample is produced by allowing the sample to settle for 12 h. Clay-sized particles remaining in suspension (c) are isolated by using a centrifuge.

### 3.1 Sample collection

In accordance with IODP procedures (see Gillis et al., 2014c), all 42 cores recovered during IODP Expedition 345 were cut in half lengthwise to produce an archive half and a working half. The sawing process cut a channel  $\sim 1.5$  mm wide in the 57 mm diameter core. The fragments produced by sawing were typically  $< 200 \mu\text{m}$  in diameter. Some fragments were up to 2 mm in diameter, and many particles were reduced to clay size. The standard procedure aboard the D/V *JOIDES Resolution* (JR) had been to discard these cuttings back to the ocean, thereby wasting the opportunity to acquire this precious and otherwise “free” sample.

Our sampling procedure on the JR was as follows: after the core was removed from its plastic casing, the core pieces were thoroughly washed and rinsed of all drilling mud using the distilled water produced on the JR. Beyond cleaning the core of contaminants, it had to be optically clean for digital imaging purposes. The samples were then cut on a new diamond saw that was enclosed on five sides by a plastic housing (Fig. 1a). Together with the spray guard at the front of the saw, all water and cuttings sprayed from the sample were contained within the housing or collected through a drain into buckets or carboys (Fig. 1b).

After all pieces in any one core (typically 0.5 to 1.5 m long) were cut, we collected all of the particles produced from sawing the slot. The coarser grains, including millimeter-sized fragments, sedimented to the bottom of the plastic housing of the saw, and as much as possible of this sedimented material was collected using a plastic spatula. Any remaining particles were collected by rinsing the shuttle, mounts, and farther reaches of the housing with a strong

spray of distilled water and capturing this rinse water through the drain into buckets or carboys (Fig. 1b). Final rinsing ensured the complete capture of all particles of all grain sizes in any given section of core. This procedure effectively collected all of the material in the 1.5 mm wide saw cut, averaged over the entire 0.5 to 1.5 m core. Furthermore, the final wash left the saw and housing clean for cutting the next section of core and for the collection of the next channel sample.

The resulting slurry of particles, or cuttings and rinse water was left to settle for at least 12 h to allow all silt-sized and larger particles (those greater than  $\sim 4 \mu\text{m}$ ) to settle to the bottom of the 37 cm tall bucket (e.g., Lewis, 1984; Fig. 1b). The supernatant suspension was then decanted from the bucket, leaving a thick slurry of particle sizes ranging from  $\sim 4 \mu\text{m}$  up to several millimeters. This slurry was then air-dried, weighed, and retained for X-ray diffraction and chemical analysis.

The suspension, then free of silt-sized particles, was passed through a  $10 \mu\text{m}$  sieve to capture any lingering coarser particles (Fig. 1c). In practice the material on the sieve never exceeded 0.1 g. This material was later added to the sedimented 4 to  $200 \mu\text{m}$  subsample. A 2 L aliquot of the remaining 5 to 35 L of suspension was then decanted into 50 mL centrifuge tubes, which were centrifuged at 2000 rpm for 10 min, removing particles  $< 4 \mu\text{m}$ . This clay-sized material was then washed in alcohol, dried in air, and weighed, producing the yield of  $< 4 \mu\text{m}$  material in grams per 2 L. The volume of the remaining suspension was then measured in a burette to  $\pm 5$  mL. Excess suspension water could then be discarded, minimizing the need to store more than a few buckets of rinse water at a time. The total mass of clay-sized particles was then calculated. The final weight of the bulk samples of each core was calculated by weighted averages of the sedimented and suspended subsamples; that is, bulk sample = suspended sample + sedimented sample.

### 3.2 X-ray diffraction

Sedimented subsamples for this analysis were reground under acetone to a fine powder using an agate mortar and pestle. Powdered samples were loaded into Ti mounts with cavities  $35 \text{ mm} \times 28 \text{ mm} \times 1 \text{ mm}$  depth and analyzed on an automated Bruker D8 diffractometer with a Cu anode and a SolX energy-dispersive detector at room temperature and  $\sim 20\%$  relative humidity. Samples were measured from  $2\text{--}70^\circ 2\theta$  with a step size of  $0.02^\circ$ . Rietveld refinements (Bish and Post, 1993) were performed using the TOPAS 5 software package (Bruker AXS). The limits of detection by XRD methods are  $\sim 1 \text{ wt}\%$  depending on the mineral and the count time used for data collection.

The Rietveld method allows for the independent refinement of modeled mineral properties, including the preferred orientations of grains in the sample mount as well as compositional parameters such as Fe / Mg occupancy in olivine, pyroxenes, amphibole, and chlorite, and the Ca / Na ratio in

plagioclase. To maximize the fit of the model to the measured diffraction signal, the effects of crystallite size and crystal strain on peak shape were also considered.

### 3.3 Loss on ignition (LOI)

Each sample was first dried for 10–12 h at 100 °C. Next, 2.5 and 0.1200 g of the sedimented and suspension subsamples, respectively, were weighed on a Mettler Toledo™ balance. Ignition at 1000 °C took place for 2 h within a Carbolite™ 1100 °C chamber furnace. The weight difference in percent between the pre-ignited powder and the ignited material is reported as loss on ignition (LOI). The 2.5 g procedure is routinely used at the Bergen Geoanalytical Facility of the University of Bergen for igneous rocks. The analytical quality control for the 0.1200 g sample material method was performed while measuring two commercially available international reference materials: basalt BIR-1 (−0.5 wt %) and gabbro MRG-1 (1.2 wt %). These data overlap with reported reference values for these materials within the GeoReM database (<http://georem.mpch-mainz.gwdg.de>, last access: 21 October 2021).

## 4 Assessment of methods and results

In the sections above, we report in detail the methods by which we collected and processed channel samples of drill core. In this section we analyze the results of our sampling in several ways to evaluate whether our methods have been appropriate, systematic, or even necessary. We follow this by exploring mineral and chemical fractionation between the sedimented and suspended subsamples, and we then compare our analyses of major elements in channel samples with those obtained by analyzing selected billets on board the JR.

### 4.1 Recovery of cuttings

To evaluate whether our sampling methods were systematic, we compare the total recovered channel sample (sedimented + suspended subsamples) with the length of core cut using data from all 42 cores. As most pieces of core were cylindrical, measurements of the length of core are a good proxy for the volume of core consumed by the cut. The correlation of the mass of sample recovered with the length of core cut (Fig. 2) is rather good with an  $R^2$  value of 0.86; the best correlation is with cores longer than  $\sim 1$  m. There is a weak correlation of length of core to total alteration, and that could explain the higher yield of grams recovered from these crumbly cores. The good correlation demonstrates that our methods were systematic, leading to a surprisingly large  $\sim 1.3$  g of sample recovered per centimeter of core cut. With a 1.5 mm slot cut into the 57 mm diameter core, the amount of material recovered is 3.3 % of the core.

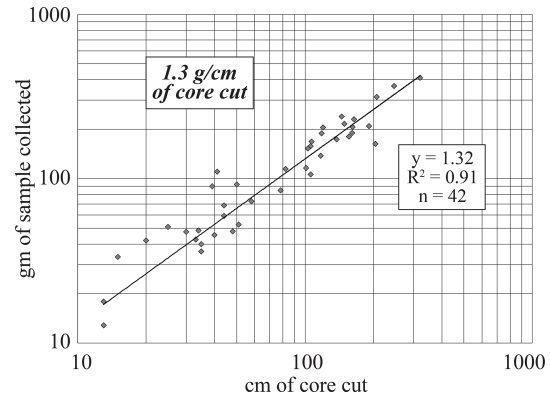


**Figure 2.** The relationship between total grams of sample collected and centimeters of core cut, illustrating that the sampling methods were systematic and that  $\sim 1.3 \text{ g cm}^{-1}$  of cut core was recovered from this process.

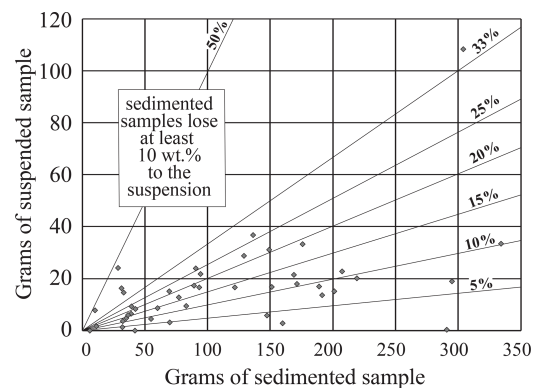


**Figure 3.** Graph comparing the weights of sedimented and suspended fractions in 42 core samples from Site 1415, Hess Deep. Equal weight fractions would follow the 50 % line. The data show that the suspended sample was generally  $> 10$  % of the total sample, but some samples produced a suspended subsample that was  $> 30$  % of the sedimented subsample.

### 4.2 Sedimented vs. suspended subsamples

To determine if collection of the suspended sediment in addition to the sedimented sample is quantitatively necessary, we compare the mass of sedimented particles recovered (Fig. 1b) with the mass of clay-sized suspended particles (Fig. 1c) for all 42 cores recovered. This comparison (Fig. 3) shows that a typical core produced between 30 and 200 g of sedimented sample. It also shows that between 5 and 40 g of suspended subsample were extracted from the suspension. This constitutes between 5 and 20 % of the total sample and over 33 % of the bulk in very short cores. There is a weak correlation between short cores and percent alteration minerals, which could explain the higher yield of suspended material in the short cores. We conclude that the relative amount of suspended material can be significant, and its collection is necessary for the characterization of the total sample.

### 4.3 Potential contamination

Several sources of contamination of our samples are possible. Cuttings created by the active drilling were flushed into the ocean with seawater and did not interfere with ship-board analyses. Cores were brought to the surface in plastic pipes, insulating them from the metal drill stems. After the core was extracted from the plastic pipe, it was thoroughly washed and rinsed with distilled water produced on board the JR. In addition to avoiding contamination, the cores needed to be devoid of particles to allow for whole-round photographic recording. We employed a new saw with new blades to eliminate contamination from samples cut on prior expeditions. The lubricating fluid for the saw was distilled water that provided no inorganic contaminants. A comparison of the concentrations of Ni vs. V (Fig. 4d) measured in our channel samples and in the billet samples shows that the range of channel sample compositions lies within the field defined by the billet concentrations. Neither data set shows outliers that could suggest contamination by any drilling or sawing tools that would contain these metals.

One last source of contamination could be the drilling mud that was used in “mud sweeps” to flush out sidewall fragments that may have fallen into the hole. To explore this possibility of contamination by drilling mud that might have survived washing of the core, we tested for the presence of Ba in the suspended and sedimented subsamples. Given the high concentration of barite in the mud, its presence would signal lingering contamination in the core. We expected barite to fractionate into the sedimented subsample because of its high density. Evidence that density contributes to fractionation between the sedimented and suspension subsamples comes from the higher concentration of Cr (Fig. 4c) and V (Fig. 4a), presumably in oxides, by up to a factor of 2 into the sedimented sample (Fig. 4c). Barium, however, does not follow this fractionation relationship. In contrast its concentration in the suspended fraction is more than 2 times that in the sedimented fraction (Fig. 4a). Furthermore, the concentrations are not larger than found in billets analyzed on board the JR (Gillis et al., 2014b, their Table T1). We infer from these results that neither barite nor drilling mud contaminated our samples (see also Sect. 4.6).

### 4.4 Mineral fractionation between suspended and sedimented samples

To determine whether any mineral fractionation occurred between the coarser sedimented subsample and the suspended clay-sized subsample, mineral modes of both size fractions were determined by X-ray diffraction and Rietveld refinement (Fig. 5). The results of these analyses show that the same suite of minerals is present in both the sediment and the suspension fractions, but that the magmatic minerals are fractionated into the coarser sedimented subsample. Plagioclase and clinopyroxene are enriched by 50 % in the sedi-

ment, whereas olivine (modeled as Fe-forsterite in the Rietveld refinement) is 2 to 5 times more abundant in the sediment. In contrast, the phyllosilicates are fractionated into the suspension. Chlorite and serpentine are nearly twice as abundant in the suspension, and talc and amphibole can be more than 5 times as abundant. Prehnite analcime and Catthomsonite show the least tendency to fractionate.

Such fractionation is not unexpected. Phyllosilicates would predictably cleave easily along their basal cleavage planes, producing thin, small-diameter platelets. These would thus dominate the clay-sized fraction in the mineralogy of the suspension. Fragments of plagioclase, clinopyroxene, and olivine with weaker or no cleavage would remain coarser and would dominate the sedimented sample. Prehnite, where abundant, might be expected to follow these magmatic minerals as it also has only one good direction of cleavage, but it fractionates into the suspended sample where it is present in low concentrations. This might be explained by its fine grain size in some samples where it is associated with plagioclase alteration (e.g., Früh-Green et al., 1996; Frost et al., 2008; Fig. 6). The conclusion from these results is that the collection of the suspended subsample is imperative to recover representative samples of these altered mafic rocks to avoid bias against the alteration minerals.

### 4.5 Chemical fractionation between suspended and sedimented samples

With the identification of the phyllosilicate fractionation into the suspended subsample, a sympathetic chemical fractionation is expected. Both FeO and MgO occur in magmatic and alteration minerals, but the phyllosilicates are concentrated in the suspended subsample. A comparison of the concentrations of these elements (Fig. 7a, b) shows no significant fractionation in olivine gabbro and troctolite in Hole P. However, in rocks from the more highly altered Hole J, FeO, MgO, Co (Fig. 4a), Eu (Fig. 4b), and Ni (Fig. 4c) do fractionate into the suspension to varying degrees. The Mg# (atomic MgO / (MgO + FeO)) is also higher in the suspended subsample, likely due to its higher concentration of serpentine (see Fig. 5). This is obvious where Mg#s of suspended and sedimented subsamples are compared (Fig. 7c). Nevertheless, the Mg# of the bulk rock is largely determined by the sedimented sample (Fig. 7d).

A comparison of CaO with Na<sub>2</sub>O concentrations shows that CaO is fractionated into the sedimented subsample (Fig. 8a), whereas Na<sub>2</sub>O is concentrated into the suspended subsample (Fig. 8b). This reflects the higher concentrations of Ca-rich plagioclase, clinopyroxene, and prehnite in the former and of Na-rich clay minerals in the latter. This interpretation is consistent with the fractionation of V, Sc, Cr, and most rare-earth elements (REEs) also into the sedimented subsamples and of Ba and Eu into the suspended fraction (Fig. 4). The modest fractionation of Sr into the sedimented sample (Fig. 4a) is a surprise given that its likely host, pla-

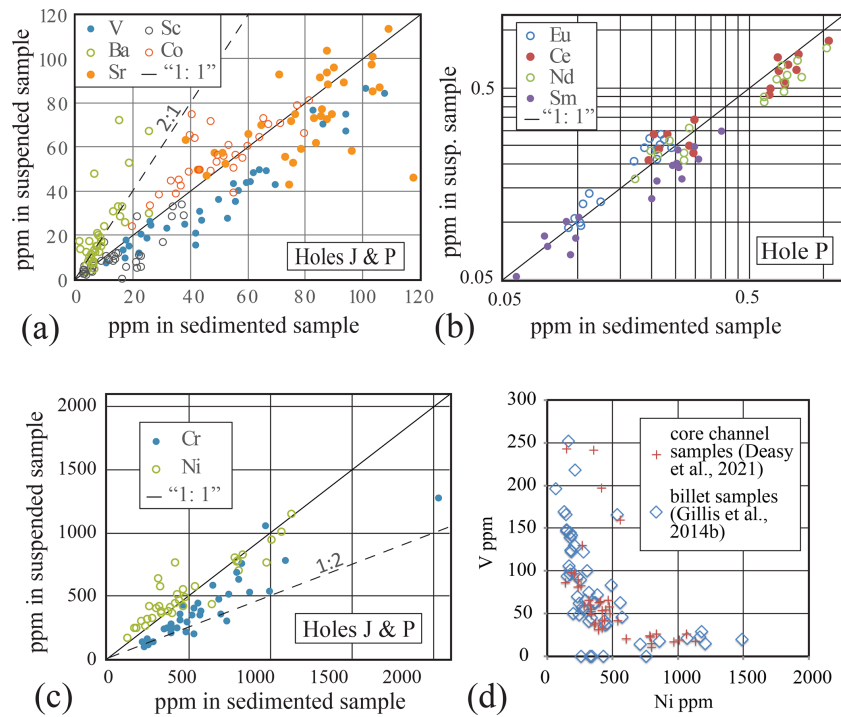


**Figure 4.** Graphs showing the distribution of selected trace elements between the suspension subsample and the sedimented subsample. (a) Ba is strongly fractionated into the suspension subsample, whereas the reverse occurs with V. (b) Little fractionation of REEs occurs with the possible exception of Eu into the suspended subsample. (c) Little fractionation occurs with Ni, but Cr is fractionated into the sedimented subsample. (d) The correlation of the concentrations of Ni and V measured in our channel samples and in the billet samples is very good, suggesting no detectable contamination in the channel samples.

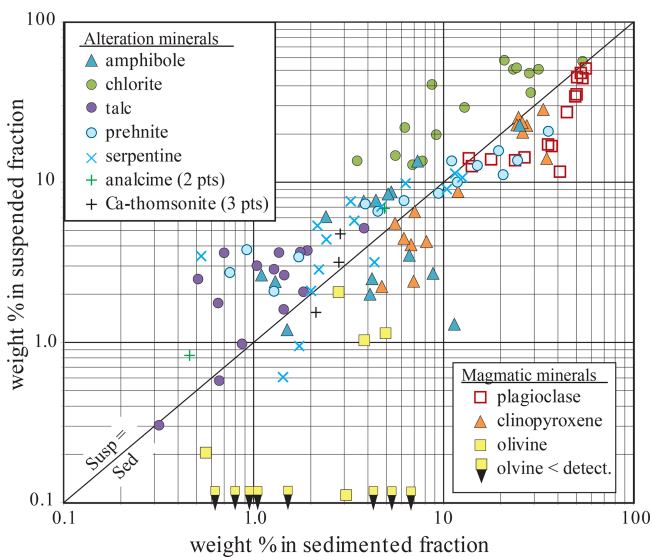


**Figure 5.** Graph comparing the weight percent (wt %) of the minerals in the sedimented subsample with the weight percent of the clay-sized minerals in the suspended subsample in cores from Hole J as determined by X-ray diffraction and Rietveld refinement. The graph shows that magmatic minerals fractionated into the sedimented subsample whereas phyllosilicates fractionated into the suspended subsample.

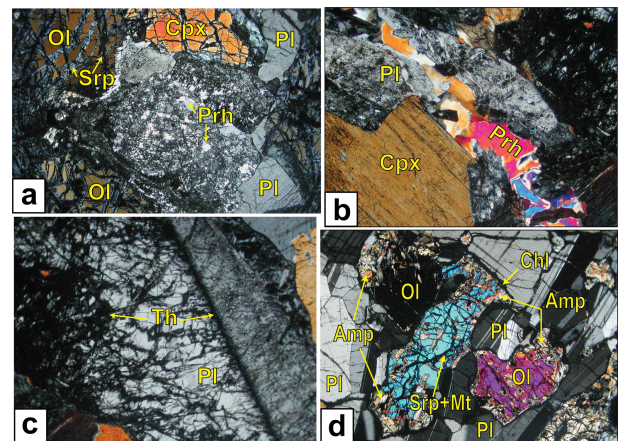


**Figure 6.** Cross-polarized light images of minerals from Hole J, Site U1415. (a) A sample of troctolite from Unit III (J19R1\_39-45), showing prehnite (Prh) replacing plagioclase (Pl) and serpentine (Srp) replacing olivine (Ol), forming a mesh texture in a plagioclase + clinopyroxene (Cpx) host. (b) A prehnite vein cutting Pl and Cpx in gabbro from Unit II (J8R3\_114-116). (c) Ca-thomsonite (Th, very low birefringence) replacing Pl in gabbro Unit II (J8R3\_114-116). (d) The alteration of Ol by amphibole (Amp) and by serpentine + magnetite (Mt) and the alteration of Pl + Ol by chlorite (Chl) in sample J7G1 44-46.

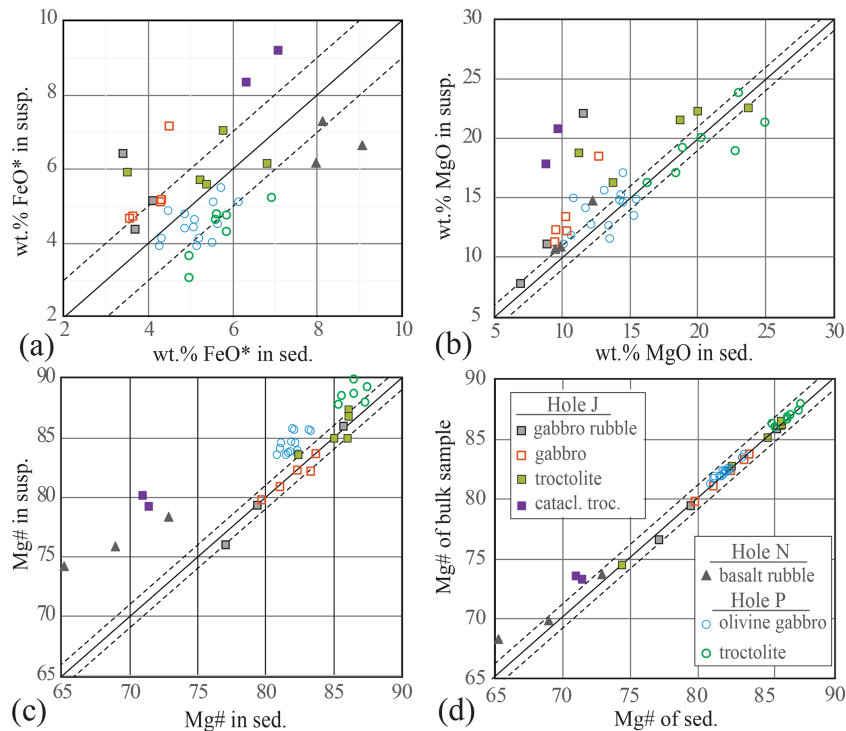


**Figure 7.** A comparison of the concentrations of MgO and FeO\* (total) in sedimented and suspended fractions of the channel samples. Solid line: 1 to 1, no fractionation. Dashed lines:  $\pm 1\%$  envelope. (a) Graph showing that there is no systematic fractionation of FeO\* between sedimented and suspended samples. (b) Graph showing that MgO tends to be fractionated into the suspended sample, reflecting the relatively high concentration of MgO-rich phyllosilicates. (c) The comparison of the Mg# between suspended and sedimented samples shows the effect of phyllosilicates raising the Mg# in the suspended sample. (d) Graph showing that the larger mass of the sedimented sample dominates the Mg# of bulk sample.

gioclase, is fractionated into the sediment (Fig. 5). The Sr content of prehnite and zeolite partially fractionated into the suspended sample probably contributes to this behavior. Figure 8c shows the corresponding higher Ca#s (atomic Ca / (Ca + Na)) in the sedimented subsample. However, as was found in the Mg system, the Ca# is dominated by the sedimented sample because of the relatively low concentration of CaO and Na<sub>2</sub>O in the suspended subsample. Consequently, the Ca# of the bulk sample follows that of the sedimented sample (Fig. 8d).

#### 4.6 Comparison of chemical compositions of channel samples and billets

We compare the chemical compositions of billets (typically  $2 \times 3 \times 3$  cm) from Hole J analyzed aboard the JR (Gilles et al., 2014b) with the chemical compositions of bulk channel samples analyzed by Deasy et al. (2021). Instrumental analytical analysis in both studies was similar with the inductively coupled plasma atomic emission spectroscopy (ICP-AES) method on the JR and ICP-AES (major elements) with inductively coupled plasma mass spectroscopy (ICP-MS, trace element) measurements reported in Deasy et al. (2021). This comparison for SiO<sub>2</sub> (Fig. 9), MgO (Fig. 10),

and two trace elements (Fig. 11) shows a general agreement between the two data sets, in spite of the differing sampling strategies. The agreement improves where averages of billet compositions are compared to the respective channel sample of the same core. In particular, the average concentrations of SiO<sub>2</sub>, MgO, Sr, and V of five billet compositions from Core 8R come close to recovering the composition of the channel sample (Figs. 9, 10, 11). The results for Sr and V from Core 8 (Fig. 11) also show that where five billets are analyzed their average more closely approaches the concentrations in the channel sample. The results also support the conclusion in Sect. 4.3 that there is no evidence for contamination in the concentration of trace elements analyzed in the channel samples.

On the other hand, individual billets are the only way to target anomalies in bulk compositions. For example, two billets from Core 13R sampled anorthosite and troctolite with very different MgO contents (Fig. 10) and moderately differing SiO<sub>2</sub> contents (Fig. 9), while the average of MgO concentration did come close to the concentration in the channel sample. Clearly, the advantage to analyzing billet-sized samples of a core is to identify heterogeneity in the composition of a core. However, the average of these local compositions

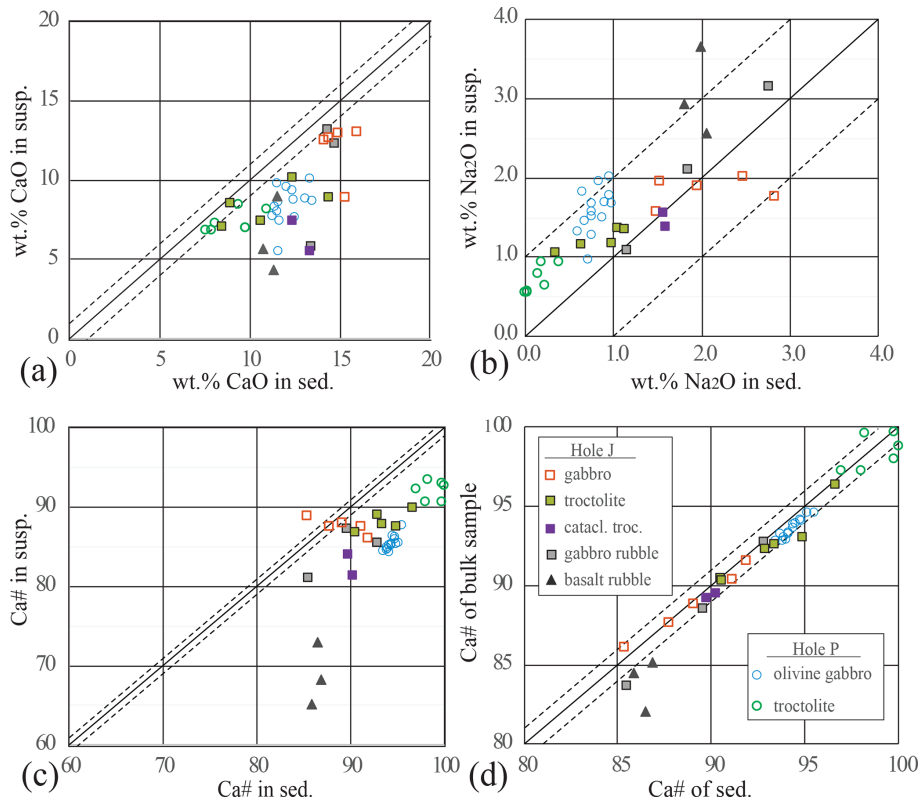


**Figure 8.** A comparison of the concentrations of CaO and Na<sub>2</sub>O in sedimented and suspended fractions of the channel samples. Solid line: 1 to 1, no fractionation. Dashed lines:  $\pm 1\%$  envelope. (a) The higher concentration of CaO in the sedimented subsample reflects the higher concentration of CaO in plagioclase, clinopyroxene, and prehnite. (b) Na<sub>2</sub>O is fractionated into the suspended subsample, reflecting its phyllosilicate host. (c) Graph showing the higher Ca# in the sedimented subsamples, consistent with the higher concentration of Ca in magmatic minerals. (d) A comparison of the Ca# in the sedimented subsample with the Ca# in the total sample. The similarity shows that the sedimented subsample dominates the Ca# in the total sample.

does not necessarily produce a representative composition of a longer length of core.

The agreement between values of loss on ignition (LOI) measured in billets with H<sub>2</sub>O calculated from crystallography is not good (Fig. 12). In this case the LOI of the billets is significantly less than the values measured for the channel samples. This relationship is probably best explained by the fact that the billets were selected for the cohesive nature of the material being sampled. By avoiding veins and altered fractures, these billets provide a better estimate of the composition of the unaltered igneous rocks. However, if the goal is to estimate the composition of a lithology as captured in the core, alteration and all, then the channel sample provides a better estimate by sampling more of the altered material. Still, the core did separate during drilling along some altered fractures and even the analyses of the channel samples gives a minimum estimate of the altered material and the LOI that would have been sampled by the full core.

#### 4.7 Correlation of modal mineralogy with geochemistry

One goal of the channel sampling described here is to analyze the bulk mineralogy and the bulk chemical composition independently. To determine if the chemical and XRD methods employed are consistent with each other, we compare their results. Unfortunately, this comparison is not straightforward, because the XRD methods with Rietveld refinement provide quantitative estimates of the wt % of each mineral and the compositions of many solid solutions. An exception is plagioclase in which the unit cell volumes of albite and anorthite differ by less than 1 %, such that X-ray peak positions are not sensitive to composition. The H<sub>2</sub>O content, however, offers an exception that does allow this comparison. The wt % of each hydrated mineral can be used to calculate the wt % of H<sub>2</sub>O in that mineral. We compare the sum of these values with the LOI for the same sample as reported by Deasy et al. (2021) in Fig. 13. The comparison does show a strong correlation but with the LOI slightly higher than the H<sub>2</sub>O calculated from crystallography. It is possible that small amounts of hydrated minerals below the detection limit of XRD methods (< 1 wt %) are present but at such a low con-

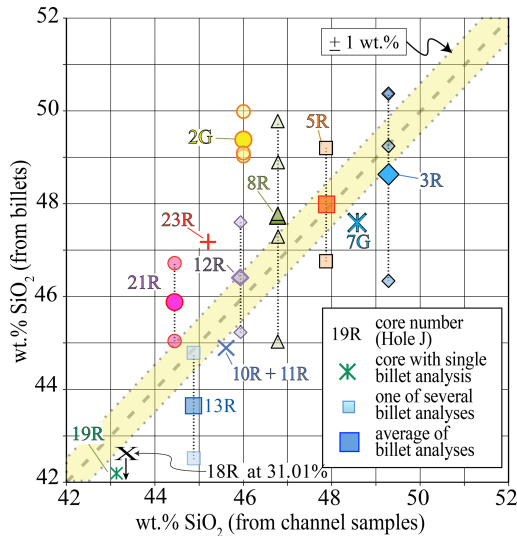


**Figure 9.** The comparison of bulk  $\text{SiO}_2$  analyses of channel samples ( $x$  axis) from core from Hole J with the analyses of billets ( $y$  axis) analyzed aboard the JR from the same cores. Where more than one billet was analyzed from a single core, they are joined by dotted vertical lines that correspond to the  $\text{SiO}_2$  concentrations of the channel samples. Average compositions of the billets are indicated by the bolder symbols. The close correspondence among many samples shows a general agreement of the two sampling methods. However, the averages or single billet compositions of 6 out of 11 samples lie outside a 1.0 wt % band (yellow), showing that average compositions of billets do not yield representative compositions of the whole core.

centration that their presence could not explain the discrepancy in Fig. 13. However, a comparison of the LOI with the actual measured  $\text{H}_2\text{O}$  on the JR (Gillis et al., 2014b, their Table T1) shows the same higher value for LOI. This demonstrates that the LOI is responding to the weight loss of not only structural  $\text{H}_2\text{O}$  but also of  $\text{CO}_2$ ,  $\text{SO}_2$ , halogens, and  $\text{H}_2\text{O}$  adsorbed on surfaces. Thus, the good fit of LOI with wt %  $\text{H}_2\text{O}$  calculated from crystallographic data supports a conclusion that each method is responding to the same material equally.

## 5 Recommendations

In order to make collection of this valuable channel sample of core more efficient and less labor intensive, we recommend the following modifications to the methods described above. The volume of water used to capture the suspended fine fraction should be minimized. This can be accomplished by recycling and filtering the (distilled) lubricating water from the bottom of the saw housing with a pump. Although rinse water for washing the saw and housing would still be required, recycling would minimize the volume of water holding the suspension by as much as 75 % for a long core. For ease in cleaning, the saw housing should be coated with Teflon.

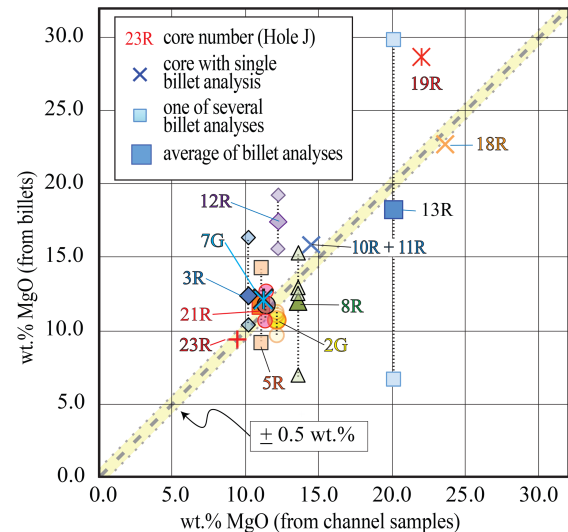


**Figure 10.** The comparison of bulk  $\text{MgO}$  concentrations of channel samples from core from Hole J with the analyses of billets analyzed aboard the JR from the same cores. The concentrations of  $\text{MgO}$  in single billets and from averages of billets from 9 out of 11 cores differ by more than 0.5 wt % (yellow band) from the compositions of the channel samples of the same cores, showing that analyses of billets do not yield representative compositions of the whole core.

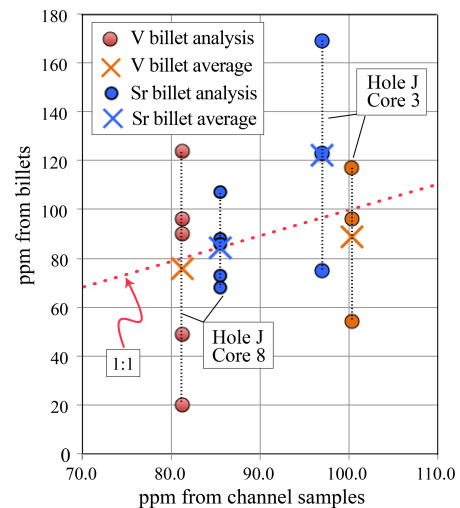


**Figure 11.** A comparison of the concentrations of Sr and V in channel samples from Cores 3 and 8 in Hole J with the analyses of billets analyzed aboard the JR from the same cores. The average concentrations of Sr and V in five billets from Core 8 approaches the concentrations in the channel sample more closely than does the average of the concentrations in three billets from Core 3.

A major rate-limiting step in sampling was the time needed for collection of the suspended material using a normal tube centrifuge. When the rate of core recovery was high, the rate of production of rinse water was much higher than could be processed by filtering and centrifuging the water.

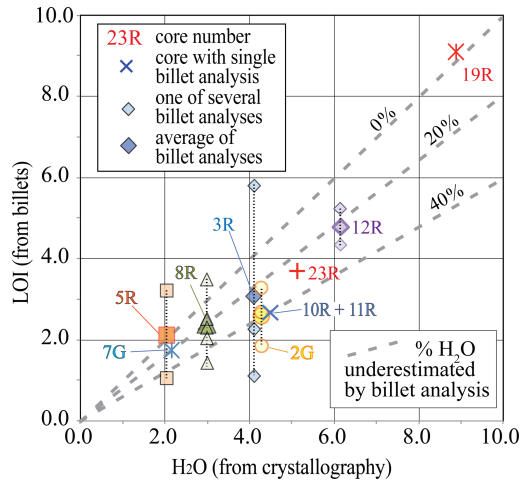


**Figure 12.** The comparison of the values of weight loss on ignition (LOI) from channel samples of the bulk cores from Hole J (this study) with values analyzed aboard the JR from billets cut from the same cores. The values of LOI from billets are as much as 40 % smaller than found in the bulk core samples.

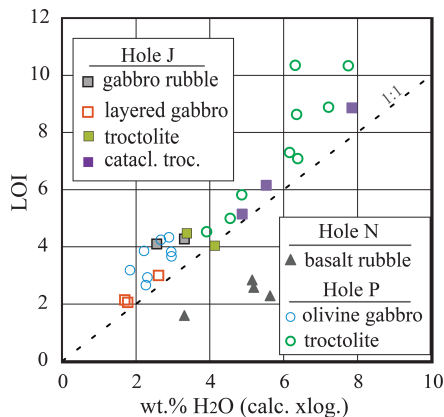


**Figure 13.** A comparison of the measured weight loss on ignition (LOI) with the wt % H<sub>2</sub>O calculated from the sum of the wt % of each hydrated mineral calculated using the Rietveld refinement (this study). The diagram shows that LOI values slightly exceed the calculated H<sub>2</sub>O contents (see text).

Use of a continuous-flow centrifuge would greatly increase the efficiency of the onboard collection of the suspended material. The slow recovery of core on Expedition 345 gave us time to collect the suspended samples, but this situation will hopefully not be repeated.

Staffing would also need to be increased. During Expedition 345, scientists from petrology and geochemistry took on double shifts to accomplish this sampling. With a greater rate of core recovery, a minimum of three scientists would be necessary for 24 h sample recovery. A fourth scientist would probably be necessary with continuous core recovery. If analytical work were to be performed on board, then one scientist would be sufficient to conduct all the XRD studies, but

three geochemists would be needed for the greatly increased number of samples to be analyzed.

Improvements in our analytical instruments are giving us ever-increasing precision in the compositions of rocks and minerals, even to the parts per trillion (ppt) levels of detection. However, without improvements in our sampling protocol, the accuracy of any analytical result will not improve. We have presented here a sampling strategy that will keep pace with advancements in analytical capabilities that will lead to both a more precise and a more accurate understanding of Earth materials in general, as well as to a deeper understanding of the mineralogical and chemical composition of the lower oceanic crust.

## 6 Discussion and conclusions

The results above show that the method of channel sampling produces a reliable, representative data set of the core involved without consuming any new split of the valuable core. In fact, the yield is a significant  $\sim 1.3 \text{ g cm}^{-1}$  of cut core (Fig. 2), a recovery of 3.3 vol % of the core. We find no evidence for contamination of our channel samples (Figs. 4, 9, 10, 11). Bulk chemical compositions of core are not attainable through an average of the compositions of subjectively selected billet-sized samples (Figs. 9, 10). An important result of this work is the discovery that there is significant mineral and thus also chemical fractionation between the sedimented material and the suspended clay-sized particles produced during cutting the core; thus, both size fractions must be sampled and analyzed to produce a representative sample of the bulk core. The collection of the suspended subsample is time-consuming, but because it commonly makes up  $> 10\%$  of the bulk sample (Fig. 3) and because phyllosilicates are selectively fractionated into it (Fig. 5), it cannot be ignored. Thus, neither the sedimented subsample nor the suspended subsample alone is representative of the bulk core composition. The results also show that the proportion of the sample in the suspension cannot be predicted, because there is no correlation between the mass of the sediment and suspended fractions. Added together, however, there is a good correlation between the total grams sampled and the centimeters of core cut (Fig. 2). Thus, the data demonstrate that only the weighted average of the two size fractions yields a representative bulk sample.

**Data availability.** The data from this research are available in Deasy et al. (2021, <https://doi.org/10.1093/petrology/egab019>).

**Author contributions.** RPW, RM, and TN designed and executed sample collection aboard the JR. RM analyzed volatile content aboard the JR, developed the wet chemistry procedure, prepared samples, and supervised the chemical analysis onshore. DLB supervised the XRD analysis and Rietveld refinements. RTD conducted

much of the chemical analysis. CJ and RTD prepared the samples and conducted the XRD analysis. Petrographic analysis was performed by TN, who also provided images in the text. RPW prepared the article with contributions from all co-authors.

**Competing interests.** The contact author has declared that neither they nor their co-authors have any competing interests.

**Disclaimer.** Any use of trade, firm, or product names is for descriptive purposes only and does not imply endorsement by the U.S. Government.

Publisher's note: Copernicus Publications remains neutral with regard to jurisdictional claims in published maps and institutional affiliations.

**Acknowledgements.** We thank the drilling and operational crew of the *JOIDES Resolution* for cooperation, as we sampled the cuttings at all hours, and the IODP Expedition 345 scientific community, especially Jon Snow for encouragement and helpful discussion aboard the JR. This work was partially supported by IODP start-up funds (grant no. 0123456). Romain Meyer was at the Centre for Geobiology, Department of Earth Science, University of Bergen, during some of this research.

**Financial support.** This research has been supported by IODP start-up funds (grant no. 0123456) and the Norges forskningsråd.

**Review statement.** This paper was edited by Thomas Wiersberg and reviewed by Thomas Belgrano and one anonymous referee.

## References

- Agterberg, F. P.: Sampling and analysis of chemical element concentration distribution in rock units and orebodies, *Nonlin. Processes Geophys.*, 19, 23–44, <https://doi.org/10.5194/npg-19-23-2012>, 2012.
- Arai, S. and Matsukage, K.: Petrology of gabbro-troctolite-peridotite complex from Hess Deep, equatorial Pacific: implications for mantle-melt interaction within the oceanic lithosphere, in: *Proc. ODP, Sci. Results*, College Station, TX (Ocean Drilling Program), edited by: Mével, C., Gillis, K. M., Allan, J. F., and Meyer, P. S., 147, 135–155, <https://doi.org/10.2973/odp.proc.sr.147.008.1996>, 1996.
- Arai, S. and Takemoto, Y.: Mantle wehrlite from Hess Deep as a crystal cumulate from an ultra-depleted primary melt in East Pacific Rise, *Geophys. Res. Lett.*, 34, L08302, <https://doi.org/10.1029/2006GL029198>, 2007.
- Bish, D. L. and Post, J. E.: Quantitative mineralogical analysis using the Rietveld full-pattern fitting method, *Am. Min.*, 78, 932–940, 1993.
- Bish, D. L., Sarrazin, P., Chipera, S. J., Vaniman, D. T., and Blake, D.: Quantitative mineralogical analysis of Mars analogues using CHEMIN data and Rietveld refinement, 35th Lunar and Planetary Science Conf., 2004: The Future of Mars Surface Exploration, 15–19 March 2004, League City, Texas, USA, 35, 1404, ID: 20040065952, 2004.
- Bish, D. L., Blake, D. F., Vaniman, D. T., Chipera, S. J., Morris, R. V., Ming, D. W., Treiman, A. H., Sarrazin, P., Morrison, S. M., Downs, R. T., Achilles, C. N., A. S. Yen, Bristow, T. F., Crisp, J. A., Morookian, J. M., Farmer, J. D., Rampe, E. B., Stolper, E. M., Spanovich, N., and the MSL Science Team: X-ray Diffraction Results from Mars Science Laboratory: Mineralogy of Rocknest at Gale Crater, *Science*, 341, 1476–1477, <https://doi.org/10.1126/science.1238932>, 2013.
- Blackman, D. K., Ildefonse, B., John, B. E., Ohara, Y., Miller, D. J., Abe, N., Abratis, M., Andal, E. S., Andreani, M., Awaji, S., Beard, J. S., Brunelli, D., Charney, A. B., Christie, D., Collins, M. J., Delacour, A. G., Delius, H., Drouin, M., Einaudi, F., Escartín, J., Frost, B. R., Früh-Green, G., Fryer, P. B., Gee, J. S., Godard, M., Grimes, C. B., Halfpenny, A., Hansen, H. E., Harris, A. C., Tamura, A., Hayman, N. W., Hellebrand, E., Hirose, T., Hirth, J. G., Ishimaru, S., Johnson, K. T. M., Karner, G. D., Linek, M., MacLeod, C. J., Maeda, J., Mason, O. U., McCaig, A. M., Michibayashi, K., Morris, A., Nakagawa, T., Nozaka, T., Rosner, M., Searle, R. C., Suhr, G., Tominaga, M., von der Handt, A., Yamasaki, T., and Zhao X.: Drilling constraints on lithospheric accretion and evolution at Atlantis Massif, Mid-Atlantic Ridge 30° N, *J. Geophys. Res.*, 116, B07103, <https://doi.org/10.1029/2010JB007931>, 2011.
- Bourdon, B., Turner, S., and Dosseto, A.: Dehydration and partial melting in subduction zones: Constraints from U-series disequilibria, *J. Geophys. Res.*, 108, 2291, <https://doi.org/10.1029/2002JB001839>, 2003.
- Coogan, L. A.: The Lower Oceanic Crust, in: *Treatise on Geochemistry*, edited by: Holland, H and Turekian, K., 2nd edn., The crust, 4.14, 497–541, ISBN 9780080959757, 2014.
- Coogan, L. A., Gillis, K. M., MacLeod, C. J., Thompson, G. M., and Hékinian, R.: Petrology and geochemistry of the lower ocean crust formed at the East Pacific Rise and exposed at Hess Deep: a synthesis and new results, *Geochem. Geophys. Geosy.*, 3, 8604, <https://doi.org/10.1029/2001GC000230>, 2002.
- Cornish, E. C.: Sampling ore deposits, *Colorado School of Mines Mineral Industries Bulletin* 9, 2, 15 pp., ISSN 0010-1745, 1966.
- Deasy, R. T., Wintsch, R. P., Meyer, R., Bish, D. L., Gasaway, C., and Heimdal, T.: Decoupling of serpentization and prehnitization in Lower East Pacific Rise Crust at Hess Deep, Fall Meeting, AGU, 15–19 December 2014, San Francisco, Calif., USA, Abs. V52A-04, Accession Number: 2016-012344, 2014.
- Deasy, R. T., Wintsch, R. P., and Meyer, R.: Bulk composition of fast-spreading oceanic crust: insights from the lower cumulates of the East Pacific Rise and from Cocos-Nazca Rift basalts, Hess Deep, *J. Petrol.* 62, egab019, <https://doi.org/10.1093/ptrology/egab019>, 2021.
- Dick, H. J. B., Natland, J. H., Miller, D. J., Alt, J. C., Bach, W., Bideau, D., Gee, J. S., Haggas, S., Hertogen, J. G. H., Hirth, G., Holm, P. N., Ildefonse, B., Iturrino, G. J., John, B. E., Kelley, D. S., Kikawa, E., Kingdon, A., Le Roux, P. J., Maeda, J., Meyer, P. S., Naslund, H. R., Niu, Y., Robinson, T. P., Snow, J. E., Stephen, R. A., Trimby, P. W., Worm, H.-U., and Yoshinobu, A.: Initial Reports, Proceed-

- ings ODP, College Station, TX (Ocean Drilling Program), 176, <https://doi.org/10.2973/odp.proc.ir.176.1999.1999>.
- Frost, B. R., Beard, J. S., McCaig, A., and Condliffe, E.: The Formation of Micro-Rodingites from IODP Hole U1309D: Key To Understanding the Process of Serpentinization, *J. Pet.*, 49, 1579–1588, 2008.
- Früh-Green, G. L., Plas, A., and Dell'Angelo, L. N.: Mineralogic and stable isotope record of polyphase alteration of upper crustal gabbros of the East Pacific Rise (Hess Deep, Site 894), in: *Proc. ODP, Sci. Results, College Station, TX (Ocean Drilling Program)*, edited by: Mével, C., Gillis, K. M., Allan, J. F., and Meyer, P. S., 147, 235–254, <https://doi.org/10.2973/odp.proc.sr.147.015.1996.1996>.
- Gillis, K. M., Coogan, L. A., and Pedersen, T. R.: Strontium isotope constraints on fluid flow in the upper oceanic crust at the East Pacific Rise, *Earth Planet. Sc. Lett.*, 232, 83–94, 2005.
- Gillis, K. M., Snow, J. E., Klaus, A., Guerin, G., Abe, N., Akizawa, N., Ceuleneer, G., Cheadle, M. J., Adrião, Á., Faak, K., Falloon, T. J., Friedman, S. A., Godard, M. M., Harigane, Y., Horst, A. J., Hoshide, T., Ildefonse, B., Jean, M. M., John, B. E., Koepke, J. H., Machi, S., Maeda, J., Marks, N. E., McCaig, A. M., Meyer, R., Morris, A., Nozaka, T., Python, M., Saha, A., and Wintsch, R. P.: Expedition 345 summary, in: *Proceedings of the Integrated Ocean Drilling Program, College Station, TX (Integrated Ocean Drilling Program)*, edited by: Gillis, K. M., Snow, J. E., Klaus, A., and the Expedition 345 Scientists, 345, 1–49, <https://doi.org/10.2204/iodp.proc.345.101.2014.2014a>.
- Gillis, K. M., Snow, J. E., Klaus, A., Guerin, G., Abe, N., Akizawa, N., Ceuleneer, G., Cheadle, M. J., Adrião, Á., Faak, K., Falloon, T. J., Friedman, S. A., Godard, M. M., Harigane, Y., Horst, A. J., Hoshide, T., Ildefonse, B., Jean, M. M., John, B. E., Koepke, J. H., Machi, S., Maeda, J., Marks, N. E., McCaig, A. M., Meyer, R., Morris, A., Nozaka, T., Python, M., Saha, A., and Wintsch, R. P.: Geochemistry summary, in: *Proc. IODP, College Station, TX (Integrated Ocean Drilling Program)*, edited by: Gillis, K. M., Snow, J. E., Klaus, A., and the Expedition 345 Scientists, 345, 7 pp., <https://doi.org/10.2204/iodp.proc.345.114.2014.2014b>.
- Gillis, K. M., Snow, J. E., Klaus, A., Guerin, G., Abe, N., Akizawa, N., Ceuleneer, G., Cheadle, M. J., Adrião, Á., Faak, K., Falloon, T. J., Friedman, S. A., Godard, M. M., Harigane, Y., Horst, A. J., Hoshide, T., Ildefonse, B., Jean, M. M., John, B. E., Koepke, J. H., Machi, S., Maeda, J., Marks, N. E., McCaig, A. M., Meyer, R., Morris, A., Nozaka, T., Python, M., Saha, A., and Wintsch, R. P.: Methods Chapter, in: *Proceedings of the Integrated Ocean Drilling Program, College Station, TX (Integrated Ocean Drilling Program)*, edited by: Gillis, K. M., Snow, J. E., Klaus, A., and the Expedition 345 Scientists, 345, 1–63, <https://doi.org/10.2204/iodp.proc.345.115.2014.2014c>.
- Gillis, K. M., Snow, J. E., Klaus, A., Guerin, G., Abe, N., Akizawa, N., Ceuleneer, G., Cheadle, M. J., Adrião, Á., Faak, K., Falloon, T. J., Friedman, S. A., Godard, M. M., Harigane, Y., Horst, A. J., Hoshide, T., Ildefonse, B., Jean, M. M., John, B. E., Koepke, J. H., Machi, S., Maeda, J., Marks, N. E., McCaig, A. M., Meyer, R., Morris, A., Nozaka, T., Python, M., Saha, A., and Wintsch, R. P.: Primitive layered gabbros from fast-spreading lower oceanic crust, *Nature*, 505, 204–207, <https://doi.org/10.1038/nature12778>, 2014d.
- Gillis, K. M., Snow, J. E., Klaus, A., Guerin, G., Abe, N., Akizawa, N., Ceuleneer, G., Cheadle, M. J., Adrião, Á., Faak, K., Falloon, T. J., Friedman, S. A., Godard, M. M., Harigane, Y., Horst, A. J., Hoshide, T., Ildefonse, B., Jean, M. M., John, B. E., Koepke, J. H., Machi, S., Maeda, J., Marks, N. E., McCaig, A. M., Meyer, R., Morris, A., Nozaka, T., Python, M., Saha, A., and Wintsch, R. P.: Proceedings of the Integrated Ocean Drilling Program; Hess Deep plutonic crust; exploring the plutonic crust at a fast-spreading ridge; new drilling at Hess Deep, Expedition 345 of the riserless drilling platform; Puntarenas, Costa Rica, to Balboa, Panama; Site U1415, 11 December 2012–12 February 2013, *Proceedings of the Integrated Ocean Drilling Program, College Station, TX (Integrated Ocean Drilling Program)*, 345, variously paginated, 2014e.
- Greenberger R. N., Harris M., Ehlmann B. L., Crotteau M., Kelemen P. B., Manning C. E., and Teagle D. A.: Hydrothermal alteration of the ocean crust and patterns in mineralization with depth as measured by micro-imaging infrared spectroscopy, *J. Geophys. Res.-Sol. Ea.*, 128, e2021JB021976, <https://doi.org/10.1029/2021JB021976>, 2021.
- Hacker, B. R., Peacock, S. M., Abers, G. A., and Holloway, S. D.: Subduction factory, 2, Are intermediate-depth earthquakes in subducting slabs linked to metamorphic dehydration reactions?, *J. Geophys. Res.*, 108, 2030, <https://doi.org/10.1029/2001JB001129>, 2003.
- Hart, S. R., Blusztajn, J., Dick, H. J. B., Meyer, P. S., and Muehlenbachs, K.: The fingerprint of seawater circulation in a 500-meter section of ocean crust gabbros, *Geochim. Cosmochim. Ac.*, 63, 4059–4080, 1999.
- Heinrichs, H. and Hermann, A. G.: *Praktikum der Analytischen Geochemie*, Springer, New York, 669 pp., ISBN 978-3-540-51874-7, 1990.
- Kelemen, P. B., Matter, J. M., Teagle, D. A. H., Coggon, J. A., and the Oman Drilling Project Science Team: *Proceedings of the Oman Drilling Project, College Station, TX (International Ocean Discovery Program)*, 19 Chapters, variously paginated, <https://doi.org/10.14379/OmanDP.proc.2020>, 2020.
- Koepke J., Abe, N., Akizawa, N., Falloon, T. J., Hoshide, T., Jean, M. M., and Snow, J. E.: IODP EXP 345: Orthopyroxene omnipresent in layered gabbros from the Hess Deep, RPR, 2013 Fall Meeting, AGU, 9–13 December 2013, San Francisco, Calif., USA, Abstract OS43A-1875, 2013.
- Lecuyer, C. and Reynard, B.: High-temperature alteration of oceanic gabbros by seawater (Hess Deep, Ocean Drilling Program Leg 147): evidence from oxygen isotopes and elemental fluxes, *J. Geophys. Res.-Sol. Ea.*, 101, 15883–15897, <https://doi.org/10.1029/96JB00950>, 1996.
- Lewis, D. W.: *Practical Sedimentology*, Hutchinson Ross Publishers, Stroudsburg, PA, 277 pp., ISBN 978-0-87933-443-7, 1984.
- Lissenberg, C. J., MacLeod, C. J., Howard, K. A., and Godard, M.: Pervasive reactive melt migration through fast-spreading lower oceanic crust (Hess Deep, equatorial Pacific Ocean), *Earth Planet. Sc. Lett.*, 361, 436–447, 2013.
- Lucia, F. J.: *Carbonate Reservoir Characterization, An Integrated Approach*, Springer, Berlin, 336 pp., ISBN 978-3-540-72740-8, 2007.
- Manning, C. E.: The chemistry of subduction-zone fluids, *Earth Planet. Sc. Lett.*, 223, 1–16, 2004.
- Manning, C. E. and MacLeod, C. J.: Fracture-controlled metamorphism of Hess Deep gabbros, Site 894: constraints on the roots of mid-ocean-ridge hydrothermal systems at fast-

- spreading centers, in: Proc. ODP, Sci. Results, College Station, TX (Ocean Drilling Program), edited by: Mével, C., Gillis, K. M., Allan, J. F., and Meyer, P. S., 147, 189–212, <https://doi.org/10.2973/odp.proc.sr.147.011.1996>, 1996.
- Manning, C. E., Weston, P. E., and Mahon, K. I.: Rapid high-temperature metamorphism of East Pacific Rise gabbros from Hess Deep, *Earth Planet. Sc. Lett.*, 144, 123–132, [https://doi.org/10.1016/0012-821X\(96\)00153-7](https://doi.org/10.1016/0012-821X(96)00153-7), 1996.
- Marks, N., Gillis, K. M., Lindvall, R. E., and Schorzman, K.: IODP Expedition 345: Characterizing Hydrothermal Alteration of Fast-Spreading EPR Lower Crust using O, Sr and Nd isotopics, 2014 AGU Fall Meeting, 15–19 December 2014, San Francisco, USA, V22A-07, 2014.38, Accession Number: 2015-088474, 2014.
- Marks, N. E., Faak, K., Gillis, K. M., McCaig, A. M., Nozaka, T., and Python, M.: IODP Expedition 345: Hydrothermal Alteration of Fast-Spreading EPR Lower Crust, 2013 AGU Fall Meeting, 9–13 December 2013, San Francisco, USA, OS43A-1879, Accession Number: 2015-070549, 2013.
- Meade, C. and Jeanloz, R.: Deep-focus earthquakes and recycling of water into the Earth's mantle, *Science*, 252, 68–72, 1991.
- Mével, C. and Stamoudi, C.: Hydrothermal Alteration of the Upper-Mantle Section at Hess Deep, in: Proceedings of the Ocean Drilling Program, Scientific Results, edited by: Mével, C., Gillis, K. M., Allan, J. F., and Meyer, P. S., chap. 15, 147, 293–309, <https://doi.org/10.2973/odp.proc.sr.147.017.1996>, 1996.
- Meyer, R., Wintsch, R. P., Nozaka, T., Gillis, K. M., and Snow, J. E., and the Scientific Crew of the Joides Resolution.: Deep fast-spread Oceanic Crust – Fluid Interactions: Petrography and Volatiles from IODP Expedition 345 Hess Deep Plutonic Crust, *Min. Mag.*, 77.5, 1750, <https://doi.org/10.1180/minmag.2013.077.5.13>, 2013.
- Natland, J. H. and Dick, H. J. B.: Melt migration through high-level gabbroic cumulates of the East Pacific Rise at Hess Deep: the origin of magma lenses and the deep crustal structure of fast-spreading ridges, in: Proceedings ODP, Scientific Results, College Station, TX (Ocean Drilling Program), edited by: Mével, C., Gillis, K. M., Allan, J. F., and Meyer, P. S., 147, 21–58, <https://doi.org/10.2973/odp.proc.sr.147.002.1996>, 1996.
- Nozaka, T. and Fryer, P.: Alteration of the oceanic lower crust at a slow-spreading axis: insight from vein-related zoned halos in olivine gabbro from Atlantis Massif, Mid-Atlantic Ridge, *J. Petrol.*, 52, 643–664, <https://doi.org/10.1093/petrology/egq098>, 2011.
- Nozaka, T., Meyer, R., Wintsch, R. P., and Wathen, B.: Hydrothermal spinel, corundum and diaspore in lower oceanic crustal troctolites from the Hess Deep Rift, *Contrib. Min. Pet.*, 171, 1–14, <https://doi.org/10.1007/s00410-016-1266-4>, 2016.
- Nozaka, T., Wintsch, R. P., and Meyer, R.: Serpentinization of olivine in troctolites and olivine gabbros from the Hess Deep Rift, *Lithos*, 282, 201–214, 2017.
- Pedersen, R. B., Malpas, J., and Falloon, T.: Petrology and geochemistry of gabbroic and related rocks from Site 894, Hess Deep, in: Proceedings ODP, Scientific Results, College Station, TX (Ocean Drilling Program), edited by: Mével, C., Gillis, K. M., Allan, J. F., and Meyer, P. S., 147, 3–19, <https://doi.org/10.2973/odp.proc.sr.147.001.1996>, 1996.
- Potts, P. J.: A handbook of silicate rock analysis, Chapman & Hall, New York, NY, USA, 622 pp., ISBN 0412008815, 1987.
- Raleigh, C. B. and Paterson, M. S.: Experimental deformation of serpentinite and its tectonic implications, *J. Geophys. Res.-Sol. Ea.*, 70, 3965–3985, 1965.
- Ranero, C. R., Villasenor, A., Phipps Morgan, J., and Weinrebe, W.: Relationship between bend-faulting at trenches and intermediate-depth seismicity, *Geochem. Geophys. Geos.*, 6, Q12002, <https://doi.org/10.1029/2005GC000997>, 2005.
- Regelous, M., Weinzierl, C. G., and Haase, K. M.: Controls on melting at spreading ridges from correlated abyssal peridotite–mid-ocean ridge basalt compositions, *Earth Planet. Sc. Lett.*, 449, 1–11, 2016.
- Sinclair, A. J. and Blackwell, G. H.: Applied Mineral Inventory Estimation, Cambridge University Press, Cambridge, 381 pp., ISBN 978-0-521-79103-8, 2002.
- Stanton, R.: Channel and core sampling of coal beds: purposes, methods, and value, Proceedings of the International Coal Testing Conference, 11–13 February 1986, Lexington, KY, USA, 63–68, Accession Number: 1992-004533, 1986.
- Stewart, M. A., Klein, E. M., and Karson, J. A.: Geochemistry of dikes and lavas from the north wall of the Hess Deep Rift: insights into the four-dimensional character of crustal construction at fast-spreading mid-ocean ridges, *J. Geophys. Res.-Sol. Ea.*, 107, 2238, <https://doi.org/10.1029/2001JB000545>, 2002.
- Stewart, M. A., Karson, J. A., and Klein, E. M.: Four-dimensional upper crustal construction at fast-spreading mid-ocean ridges: a perspective from an upper crustal cross-section at the Hess Deep Rift, *J. Vol. Geoth. Res.* 144, 287–309, <https://doi.org/10.1016/j.jvolgeores.2004.11.026>, 2005.
- Swanson, V. E. and Huffman Jr., C.: Guidelines for Sample Collecting and Analytical Methods Used in the U.S. Geological Survey for Determining Chemical Composition of Coal, US Geological Survey Circular 735, 18 pp., ISSN 03646017, 1976.
- White, W. M. and Klein, E. M.: Composition of the Oceanic Crust, in: Treatise on Geochemistry, 2nd edn., edited by: Holland, H. and Turekian, K., The crust, 4.13, 457–492, ISBN 978-0080448473, 2014.
- Wintsch, R. P., Bish, D. L., and Meyer, R.: IODP Expedition 345: Bulk Mineralogy From Lower Oceanic Crustal Rocks of the Hess Deep, in: 2013 AGU Fall Meeting, 9–13 December 2013, San Francisco, USA, OS43A-1880, Accession Number: 2015-070550, 2013.
- Wintsch, R. P., Deasy, R. T., Bish, D. L., and Meyer, R.: Stepped alteration of lower oceanic crust at Hess Deep from whole rock  $^{87}\text{Sr}/^{86}\text{Sr}$  data and quantitative modal mineralogy, in: AGU Fall Meeting, 9–13 December 2019, San Francisco, USA, V33E-022, 2019.